Demonstration of the feasibility and practical value of direct acoustic measurements in liquid metals

[1]*Kazhikenova S.Sh., [1]Shaikhova G.S., [1]Shaltakov S.N., [2]Belomestny D.

[1] Abylkas Saginov Karaganda Technical University, Karaganda, Kazakhstan
[2] Duisburg-Essen University, Duisburg, Germany

* Corresponding author email: sauleshka555@mail.ru

ABSTRACT

The temperature dependences of ultrasound absorption and propagation speed in simple semimetals, semiconductors, and semiconductor compounds have been studied in this article. Experimental and theoretical results testify to the microheterogeneity of semimetals and semiconductor melts. Generalization and analysis of experimental data on the absorption and propagation speed of ultrasound in melts based on D.I. Mendeleev periodic law clearly indicate the presence of micro-groups of atoms (clusters) in them, microheterogenizing melts of semimetals and semiconductors. The urgency of this problem is predetermined by the problem of the liquid state of matter. The dependence of ultrasound absorption and propagation speed on temperature is measured using several groups of samples in paper, each group is heated to a different temperature. It is proved that melts have clustered in their atomic matrix, and so melts with semiconductor properties are micro-inhomogeneous. These results are needed to scale melt sonication to an industrial scale and are needed to provide valuable new insights into temperature dependencies of ultrasound absorption.

Keywords: melts, atomic mass, ultrasonic melt, ultrasound absorption, temperature dependences, ultrasound propagation speed.

Kazhikenova Saule Sharapatovna	Doctor of Technical Sciences, Professor, Head of the Higher Mathematics Department of Abylkas Saginov Karaganda Technical University, Karaganda city, 100027, Nursultan Nazarbayev Avenue, 56. E-mail: sauleshka555@mail.ru
Shaikhova Gulnazira Serikovna	Candidate of Engineering Sciences, acting associate professor of the Higher Mathematics Department of Abylkas Saginov Karaganda Technical University, Karaganda city, 100027, Nursultan Nazarbayev Avenue, 56. E-mail: shaikxova_2011@mail.ru
Shaltakov Sagyndyk Nagashibayevich	Ph.D., acting associate professor of the Physics Department of Abylkas Saginov Karaganda Technical University, Karaganda city, 100027, Nursultan Nazarbayev Avenue, 56. E-mail: sagyndyk613@mail.ru
Belomestny Denis	PhD, Professor University of Duisburg-Essen, Forsthausweg 247057 Duisburg, Universitätsstraße 245141, Germany. E-mail: denis.belomestny@uni-due.de

Introduction

Semiconductor physics, including its technical applications, was limited to polycrystalline and rarely amorphous materials (such as selenium) until the middle 1940s. This was the time when the semiconductors theory foundations were laid, including the development of Wilson's impurity conductivity model and Schottky's theory of barrier layer. The subsequent development of semiconductor physics, physical chemistry, and related sciences has led to the fact that the use of liquid semiconductors in electronics as a raw material for microelectronics currently goes hand in hand with the new single-crystal materials growth and development, especially when creating high-speed processors for computer technology.

The hypothesis of the liquid's micro-heterogeneous structure arose as early as the 1920s. in connection with liquids using X-rays Stewart's studies [1]. Since then, this hypothesis has won many adherents among researchers. Methods have been developed for estimating the size of microheterogeneity, their volume fraction [[2], [3]], and calculating coordination numbers [4]. The special distinction was not between the melts of metals and semiconductors in this case. Micro-inhomogeneity extended to any melts from alkali metals to semiconductors. However, without having unambiguously interpreted experimental evidence, the hypothesis remained and had not only

adherents but also opponents. Among the works that deny the polycrystalline model of liquids is the work by a reference [5]. They are more inclined to see a fluctuation basis in individual phenomena.

A large number of works have been devoted to the study of electronic melts. Among them, the most ambitious are the extensive studies with employees of electrophysical, volumetric, viscometric, and acoustic studies [[6], [7]].

Recently, the study of liquid semiconductors, which is the subject of this work, continues to expand continuously due to progress in solid-state physics and semiconductor technology, as well as physical chemistry. In this case, structural research is of particular importance.

Ultrasonic processing is important and interesting. This is needed as a promising route to improving melt quality for scientific and industrial problems. The significance of this problem is predetermined by the matter liquid state problem. In this study, the ultrasound absorption and propagation speed and temperature are measured using multiple groups of melts and semiconductors, that were not widely also studied, since the high-temperature acoustic experiments technology with aggressive melts of semimetals and semiconductors complicated the research process. This study summarizes the results of the evaluation of ultrasound absorption and the propagation speed, for calculating the ultrasound propagation speed in solutions, studies of the nucleation, growth, and fragmentation of particles in liquid melts. It has been proven that melts with semiconductor properties are micro-inhomogeneous due to the existence of clusters in their atomic matrix. These results are needed to scale melt sonication to an industrial scale and are needed to provide valuable new insights into temperature dependences of ultrasound absorption and propagation speed in simple semimetals, semiconductors, and semiconductor compounds that have been studied by the authors. The application of absorption and propagation speed waves in electron melts is quite complex, and their interpretation requires the use of several mechanisms to describe process power, and the mechanical and microstructures properties [8]. In fact, the entire arsenal of modern experimental and theoretical physics is connected to the research of the physicochemical behavior of melts [[9], [10], [11], [12]]. Acoustic methods are the most promising among experimental methods for research of the matter liquid state. They are simple, reliable, and highly sensitive to changes in matter structure and interatomic interaction.

The application of power ultrasound during liquid-to-solid transformation is believed to be an effective way to improve the solidification microstructures and mechanical properties [8]. In fact, the entire arsenal of modern experimental and theoretical physics is connected to the research of the physicochemical behavior of melts [9]. Acoustic methods are the most promising among experimental methods for research of the matter liquid state. They are simple, reliable, and highly sensitive to changes in matter structure and interatomic interaction.

The results of this research make it possible to predict the melt's elastic properties of simple substances and extend it to complex substances.

At present, the electrophysical, thermophysical, thermodynamic, and viscous properties of liquid semimetals and semiconductors based in the electronics industry have been widely studied.

However, the ongoing research in the field of studying these properties is not sufficient to solve the problem of the liquid semimetals and semiconductors structure. It is also impossible to obtain an unambiguous result by only structural research. In this aspect, it is known that «modern acoustic research methods are a powerful tool for obtaining information about the structure of melts and semiconductors» [10]. Melts and semiconductors were not widely also studied, since the high-temperature acoustic experiments technology with aggressive melts of semimetals and semiconductors complicated the research process [[8], [9], [10], [11], [12], [13]]. Our research includes
- the development of liquid semimetals and semiconductors structure model;
- experimental and theoretical studies of the propagation speed and absorption coefficient of ultrasound temperature dependences in liquid semimetals and semiconductors;
-regularities generalization of liquid metals, semimetals, and semiconductors structural properties.

The ultrasound absorption and propagation speed waves in electron melt are quite complex, and their interpretation requires the use of several mechanisms to describe this process. For example, to interpret the experimental dependence of the sound absorption coefficient in liquid sulfur, the authors of [64±67] used the relaxation theory [14],

which assumes a micro inhomogeneous structure of highly viscous liquids.

The $\frac{\beta}{f^2}$ polytherms behavior in the after-melting temperature range is associated with relaxation mechanisms in the high-temperature region by the authors, where the speed has a maximum value and the ultrasound absorption coefficient is minimal. The sound absorption coefficient practically does not change at higher temperatures, despite the fact that the speed has a minimum value.

It was noted in a reference [15] that $\frac{\beta}{f^2}$ depends on the frequency, namely, as the sound frequency increases, the absorption coefficient decreases. However, in a reference [16], in contrast to the reference [15], no frequency dependence was observed. The sound absorption value in liquid sulfur is proportional to the frequency square, i.e. $\beta \sim f^2$. The experimental ultrasound absorption coefficient exceeds the classical value 2 times, while in the reference [16] this process excess is 3 times.

The ultrasound absorption in liquid binary systems was studied by Abovitz and Gordon [17], where $\frac{\beta}{f^2}$ was measured for the first time in the mercury ± thallium system. As the authors of this work pointed out, the low melting point of the components of this system allowed them to operate at a high frequency (up to 270 MHz).

The ultrasound absorption coefficient in the mercury-thallium alloy decreases with increasing frequency, which indicates the presence of relaxations. The $\frac{\beta}{f^2}$ value decreases with increasing temperature and increases with increasing thallium concentration.

The authors conclude that the relaxation that occurs in mercury-thallium alloys under the periodic stresses action is a structural relaxation associated with a change in the average number of nearest neighbors of both types surrounding a given atom. Relaxation is characterized by diffusion rates.

Dzharzinsky and Litovits [18] showed that in melts of the *K-Na* system, the $\frac{\beta}{f^2}$ value increases as a temperature 473–673 K function at 30 and 70 MHz frequencies.

At the same time, the authors of the reference [15] at 30 MHz frequencies obtained the opposite sound absorption polytherm than at the same frequency. Perhaps this is due to the acoustic contact instability between the melt and the sound ducts. However, at higher temperatures, good agreement is observed between the experimental results of [15] and [19].

The work [19] also presents a relaxation sound absorption theory in associated liquids. Theoretical results qualitatively correctly describe the behavior of the absorption polytherm coefficient. Quantitatively, the sound absorption coefficient theoretical value differs by almost 100% from the experimental results.

The ultrasound absorption measurement in liquid sulfur was carried out in [15]. As is known from X-ray data, liquid sulfur consists of ring formations. Apparently, these features affect such liquid sulfur characteristics as viscosity and sound propagation speed. The sound speed polytherm in molten sulfur shows three regions with different sound speed temperature coefficients. The same feature is inherent in the sound absorption polytherm in molten sulfur [15]. The studies were carried out with high-purity sulfur at a 30–60 MHz frequency in the temperature range from the melting point to 673 K.

The $\frac{\beta}{f^2}$ temperature dependence is quite complex, there is a decrease in the ultrasonic wave absorption coefficient immediately after melting, which increases monotonically with increasing temperature. This includes the alkali metals and further all other simple metals that are densely packed in the solid state.

Two-component liquid-metal solutions with monotonically increasing ultrasound absorption polytherms should also be attributed to this class.

The second class includes melts in which the ultrasonic waves absorption polytherms do not increase monotonically with temperature. This class includes semimetals and semiconductors, which undergo significant structural changes during melting.

All melts with anomalous behavior of absorption polytherms and propagation rates (bismuth, antimony, tellurium, etc.) are characterized by the fact that structural changes in them continue in a certain temperature range after melting. This is especially pronounced in melts of tellurium, antimony, etc. The $\frac{\beta}{f^2}$ anomalous behavior temperature interval of these melts coincides with the after-melting temperature range [6].

Such a classification can be given for sound speed polytherms in electron melts. A similar classification of polyterms v_s is given in a reference [6]. According to their data, polytherms of ultrasonic propagation speed in *AlSb*, *GaSb*, and *InSb* melts can be assigned to the second class [6]. In these semiconductor compounds, an increase in the ultrasound speed is observed in the after-melting temperature range.

Thus, an available data analysis of the acoustic properties of experimental studies of electron melts shows that the behavior of the ultrasonic wave absorption polytherm and propagation speed is characterized by anomalies and features of semimetal and semiconductor melts acoustic properties.

This was the reason for separating these melts into electron melts separate classes. The entire set of experimental data on speed, density, and electrical properties [6], as well as the results of structural studies [7], show that this electron melts class exhibits changes in the short-range order structure upon heating.

Therefore, anomalies and features of melts, semimetals, and semiconductors' acoustic properties should be considered manifestations of structural changes.

Results and discussion

A hypothesis about the micro-inhomogeneous structure of liquids arose in connection with Stuart's research using X-rays in 1920. Micro-inhomogeneity extends to any melts from alkali metals to semiconductors. But the hypothesis remained a hypothesis since there were no interpreted experimental data. The ultrasonic generator used for experiments to any melts from alkali metals to semiconductors were interpreted experimental data.

Experimental and theoretical results testify to the microheterogeneity melts, which were interpreted for any melts by Doppler velocimetry.

Authors of this study solved different problems to obtain sufficient Doppler signals.

The first is the ultrasonic transmission through the channel wall of steel. The second is to obtain the acoustic coupling with the channel wall, and the next one is to wett of the inner surface of the wall by the melts.

The ultrasound Doppler velocimetry method with DOP3000 Velocimeter (Figure 1) was used in

order to measure the acoustic flow investigation and flow velocities. The ultrasound Doppler velocimetry method has become an accepted method for obtaining acoustic flow investigation as shown for example in a reference [20].

With the DOP3000 there was a measurement of the speed of sound in melts by accurately measuring time, by means of an ultrasonic pulse measured over the measurement.

Before using the software, firstly, we install the probe as defined in the Figure 1. We placed the probe at a defined distance (Dmes) from a reflector on Figure 2. The reflector is a plan surface, placed perpendicularly to the US beam axis of the probe. The probe is completely immerged. The distance between the reflector and the probe surface (Dmes), which is named "Reference distance" in UDOP, must be in the range 15 to 50 mm and must be measured with precision as any error in the measured distance will be directly transferred to the sound speed measured value.

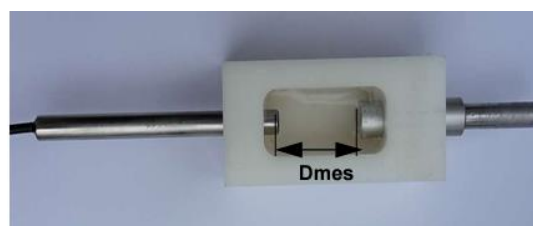**Figure 1** - The DOP3000 Velocimeter

Figure 2 - The probe

The propagation of elastic waves is associated with the fundamental properties of material media, including the mass of particles, their space, and the bonds between particles of matter. These indicators, namely, the inertial factor (mass of particles), the spatial factor (volume per particle), and the stiffness factor between particles (compressibility) are sufficient for a general description of elastic waves absorption and propagation speed [13]. First of all, this is the relationship of the selected factors with the absorption coefficient of ultrasonic waves.

For the occurrence of such observations in the behavior of the melts' elastic properties, one can use the system analysis methods based on the D.I. Mendeleev Periodic phenomenon.

As is known, the absorption coefficient is determined by the Stokes-Kirchhoff formula in the general case [21]:

$$\beta = \frac{2\pi^2 f^2}{\rho v_s^3} \frac{4}{3}\eta + \chi\left(\frac{1}{C_V} - \frac{1}{C_P}\right),$$

χ - is the thermal conductivity coefficient, C_P and C_V equal the heat capacity at constant pressure and volume.

The Stokes-Kirchhoff formula will take the form after the replacement $\gamma = \frac{C_P}{C_V}$:

$$\beta V_A = \frac{2\pi^2 f^2}{\rho v_S^3}\left[\frac{4}{3}\eta + \frac{\chi}{C_P}(\gamma - 1)\right] \qquad (1)$$

Formula (1) will be transformed to inertial, coupling and spatial factors based on the parameters $\eta = \rho\upsilon$, υ is the kinematic viscosity, $\frac{1}{\rho v_S^2} = \alpha_S$ is the adiabatic compressibility, $C_P = \frac{dQ}{dT}\frac{1}{m}$ is the melt heat capacity:

$$\frac{\beta v_S}{f^2} = 2\pi^2 \alpha_S \left[\frac{4}{3}\rho\upsilon + \frac{\chi}{\left(\frac{dQ}{dT}\right)_P} m(\gamma - 1)\right]. \qquad (2)$$

Let $\rho = \frac{m}{V} = \frac{N_A M_A}{N_A V_A}$ and $m = N_A M_A$, N_A is the

Avogadro number, M_A is the atomic mass, V_A is the atomic volume. Then we rewrite equality (2) in the form:

$$\frac{\beta v_S}{f^2} = \sigma M_A, \qquad (3)$$

$$\sigma = 2\pi^2 \alpha_S \left[\frac{4}{3}\frac{\upsilon}{V_A} + \frac{\chi}{\left(\frac{dQ}{dT}\right)_P} N_A(\gamma - 1)\right].$$

The obtained equation (3) makes acoustic parameters monitoring in simple substances melts more accessible. Experimental measurements monitoring by value using reference data [[22], [23], [24], [25], [26]] is shown in Figure 3.
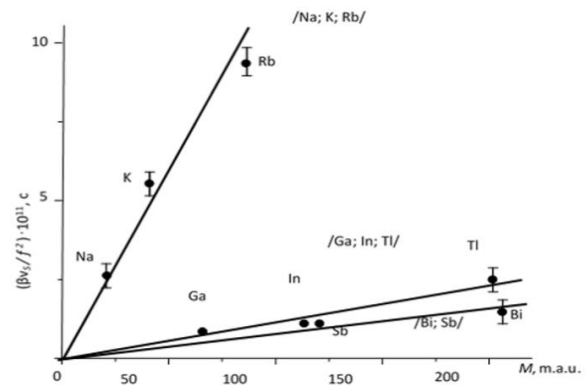

Figure 3 - Dependence at crystallization temperatures

We have established the correlation dependence between measurement results $\frac{\beta v_S}{f^2}$ and the parameter values M_A, where σ is a constant value for each group. Note: the bonding factors intragroup similarity is not only observed in condensed bodies but also in diatomic molecules.

The highest value of the dissociation energy is observed for five electrons in the outer shell, the most rigid bonds exist in diatomic molecules [27].

Local bonds become stronger (partial atomic association) with an increase in the number of external electrons in melts due to electron redistribution. There is no redistribution of electrons in diatomic molecules since they bond with a single direction from one atom to another. If the number of external electrons is more than five in diatomic molecules, then individual electrons are transformed into a non-bonding state. This situation is explained by a decrease in the dissociation energy of diatomic molecules, starting from the oxygen group [27]. The closest packing coordination number (the number of bonds realization directions) can reach twelve in condensed matter. If there are more electrons than necessary to implement a uniform bond, they are redistributed. As a result, bonds more rigid are formed between individual neighboring atoms, associations of atoms are created.

It should be noted that the weakening of bonds between associates leads to an increase in bonds in associates and a decrease in the overall rigidity of the melt macroscopic volume. This is confirmed by the sulfur group example. There is a high correlation between the parameter $\frac{\beta v_S}{f^2}$ and the atom associates in the liquids of this group. The experimental values will be equal for *S*, for *Se*, for *Te*:

$$\frac{\beta v_S}{f^2} = 19 \cdot 10^{-11} c, \quad \frac{\beta v_S}{f^2} = 6{,}7 \cdot 10^{-11} c, \quad \frac{\beta v_S}{f^2} = 1{,}34 \cdot 10^{-11} c$$

which indicates a decrease the atom associates in *S, Se, Te* melts.

Figure 3 showed that the parameter $\dfrac{\beta v_S}{f^2}$ increases from *Na* to *Rb* in the alkali metal series. This is confirmed by the fact that these groups of metals are prone to structure loosening with increasing atomic mass M_A.

The $\dfrac{\beta}{f^2}$ temperature dependence is quite complex. Immediately after melting, there is a decrease in the absorption coefficient of ultrasonic waves, which increases monotonically with increasing temperature. This includes the alkali metals and further all other simple metals that are densely packed in the solid state.

Two-component liquid-metal solutions with monotonically increasing ultrasound absorption polytherms should also be attributed to this class. The absorption coefficient of ultrasonic waves decreases immediately after melting. In addition, the absorption coefficient of ultrasonic waves increases monotonically with increasing temperature. This includes the alkali metals and further all other simple metals that are densely packed in the solid state. Melts, in which the absorption polytherms of ultrasonic waves do not increase monotonically with temperature, belong to the second class. This class includes semimetals and semiconductors, in which significant structural changes occur during melting. All melts with anomalous behavior of absorption polytherms and propagation rates (bismuth, antimony, tellurium, etc.) are characterized by the fact that their structural changes continue in a certain temperature range after melting.

This is especially pronounced in tellurium, antimony melts, etc.

The polytherm $\dfrac{\beta}{f^2}$ anomalous behavior temperature interval of these melts coincides with the "after-melting" temperature interval. The experimental results of equation (3) can be also used for compounds. For monitoring, let us consider *GaSb* and *InSb* compounds.
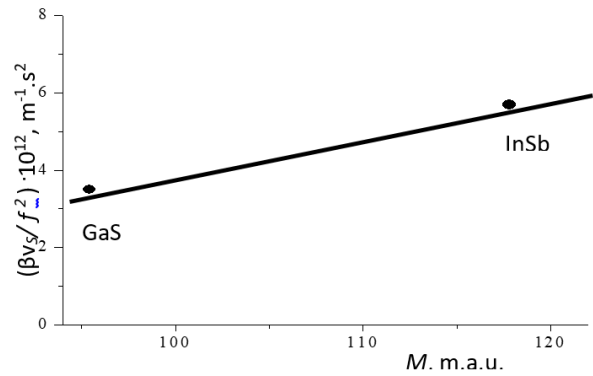

Figure 4 - Dependence   for *GaSb* and *InSb* systems

Dependence $\dfrac{\beta v_S}{f^2} - M$ is shown in Figure 4 for these compounds.

Thus, the acoustic analysis in electron melts experimental measurements shows that the absorption polytherms and the propagation velocity behavior of ultrasonic waves depend on the semimetals and semiconductors' acoustic properties. This was the reason for separating these melts into an electron melts separate class.   A straight-line relationship between $\dfrac{\beta v_S}{f^2}$ and M_A inertial factor has been established.

For calculations, melt compounds were rotated by acoustically equivalent liquids from atoms of the same type by mass that satisfies the condition

$$M = M_1 X_1 + M_2 X_2, \tag{4}$$

M_1, M_2 - atoms mass; X_1, X_2 - components atomic fractions.

The experimental results of equation (3) can be used for compounds, too. Let us consider *Bi-Sb* compound. Methods of descriptive statistics were used to systematize and describe the data. Experimental measurements monitoring by value using reference data [[22], [23], [24], [25], [26]] is shown in Figure 3. The experimental results are shown in Figure 4-14 for *GaSb* and *InSb*, $Bi_{0,25}Sb_{0,75}$, $Bi_{0,5}Sb_{0,5}$, $Bi_{0,75}Sb_{0,25}$, *Bi-Sb*, $Sn_{0,30}Te_{0,70}$, $Sn_{0,5}Te_{0,5}$, $Sn_{0,70}Te_{0,30}$, *Sn-Te* compounds. We used the Table 1 experimental measurements to build a Figure with markers in Excel.

Table 1 - Temperature dependence of Ultrasound absorption and propagation speed

T, К	$\frac{\beta}{f^2}\cdot 10^{15}$	ν_s	T, К	$\frac{\beta}{f^2}\cdot 10^{15}$	ν_s	T, К	$\frac{\beta}{f^2}\cdot 10^{15}$	ν_s
Ga			**Bi**			**Te**		
302	2.2	2866	526	9.2	1640	734	14.5	935
325	2.9	2868	545	9.3	1643	750	14.2	955
335	3.3	2870	565	9.5	1641	762	13.8	980
370	3.5	2865	599	9.8	1639	730	13.2	990
395	3.1	2860	610	9.9	1639	812	13	1015
405	3.4	2854	615	10	1638	830	12.9	1035
425	2.8	2853	630	10.3	1636	862	13	1045
450	2	2856	635	10.7	1636	883	13.1	1050
475	1.4	2858	660	10.8	1633	902	13.2	1060
500	1.2	2853	710	11.1	1630	912	13.3	1075
520	1.2	2847	730	11.3	1627	992	13.5	1090
545	1.22	2844	735	11.7	1621	974	14.1	1100
575	1.18	2848	740	12	1620	1006	15.1	1110
585	1.28	2849	755	12.4	1619	1051	17	1120
595	1.3	2841	770	12.9	1617	1078	17.5	1125
SnTe			**Se**			**Sb**		
1211	22.8	1533	520	725	1087	902	5.45	1902
1213	23.3	1531	526	635	1075	918	5.28	1911
1220	23.5	1528	544	630	1063	945	5.2	1915
1226	24	1526	560	665	1043	960	5.44	1914
1229	23.8	1522	574	565	1030	970	5.6	1913
1239	24.4	1523	620	610	1018	986	5.8	1917
1247	25.5	1520	624	680	1005	1000	5.83	1920
1254	27.9	1517	652	735	995	1020	6.4	1922
1262	29	1516	682	825	980	1035	6.5	1920
Bi₂Se₃			**Ga₂Te₃**			**Sb₂Te₃**		
1000	33	1398	1065	902	1156	902	24.4	1225
1005	32.01	1395	1075	909	1152	909	23.1	1230
1018	30.7	1390	1085	923	1151	923	22	1235
1025	30	1385	1097	933	1146	933	21	1238
1037	29.3	1368	1110	948	1142	948	18.5	1239
1045	28.8	1360	1112	969	1140	969	16.5	1244
1049	28.7	1358	1130	983	1141	983	15	1251
1060	28	1357	1148	1007	1174	1007	14.1	1251.5

Table 1 - continuation

1070	27.8	1350	1160	1030	1139	1030	13.8	1256
1074	27.7	1354	1185	1049	1156	1049	14	1258
InTe			**Sn**			**In**		
980	19.6	1156	500	4.8	2478	440	4.3	2307
990	19.01	1152	560	5.4	2472	462	4.4	2301
948	18.5	1151	584	5.1	2463	500	4.8	2295
1010	18	1146	619	5	2464	520	5	2290
1025	17.5	1142	680	6.5	2473	570	5.9	2278
1040	16.9	1140	740	9.5	2450	598	6.9	2264
1050	16.6	1141	820	10.5	2445	625	7.3	2250
1060	16.4	1174	880	12	2414	640	7.8	2242
1070	16.2	1139	940	12.4	2404	675	8.6	2232
Bi $_{0,75}$ Sb $_{0,25}$			**Sn $_{0,3}$ Te $_{0,7}$**			**Sn $_{0,7}$ Te $_{0,3}$**		
670	7.5	1698	868	18.5	1452	984	11.4	1929
690	9.5	1694	890	18.4	1449	995	11.7	1926
710	12.8	1690	910	19.5	1446	1020	12	1921
730	17	1688	938	20.6	1441	1045	12.2	1920
745	19.8	1687	980	21	1438	1050	12.7	1917
775	25.5	1684.5	1020	23	1428	1080	14	1912
800	30.1	1679	1060	24.8	1425	1087	14.5	1908

Dependence $\dfrac{\beta v_S}{f^2} - M_A$ is shown in Figure 5-7

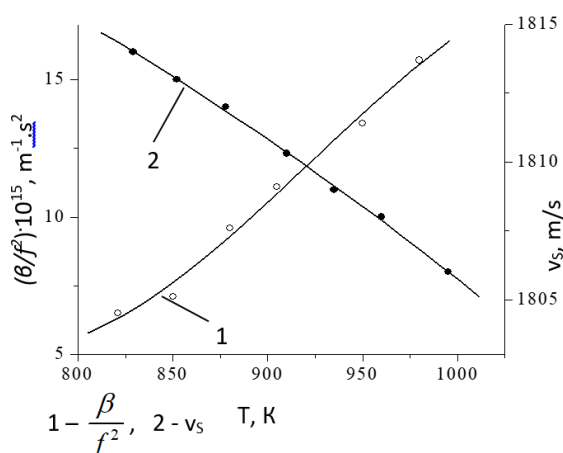for these $Bi_{0,25}Sb_{0,75}$, $Bi_{0,5}Sb_{0,5}$, $Bi_{0,75}Sb_{0,25}$ compounds.

$1 - \dfrac{\beta}{f^2}$, $2 - v_S$ T, К

Figure 5 - Temperature dependence in the $Bi - Sb$ system (composition $Bi_{0,25}Sb_{0,75}$)
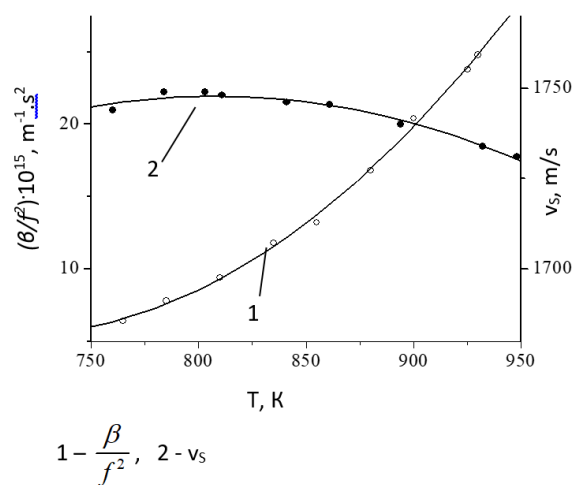

$1 - \dfrac{\beta}{f^2}$, $2 - v_S$

Figure 6 - Temperature dependence in the $Bi - Sb$ system (composition $Bi_{0,5}Sb_{0,5}$)

Figure 7 - Temperature dependence
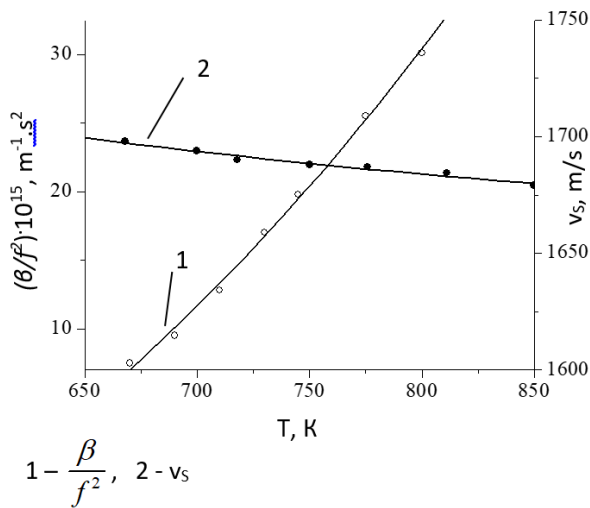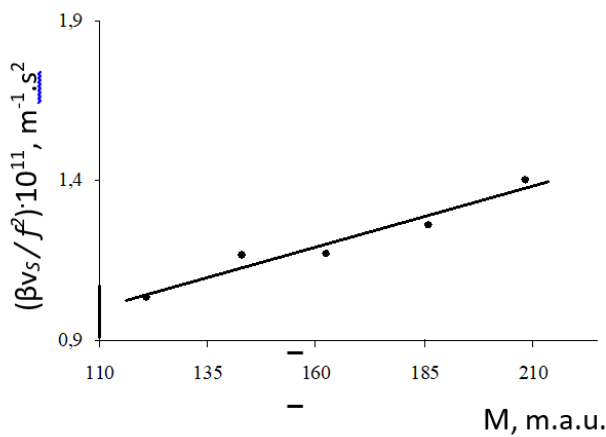in the $Bi - Sb$ system (composition $Bi_{0,75}Sb_{0,25}$)

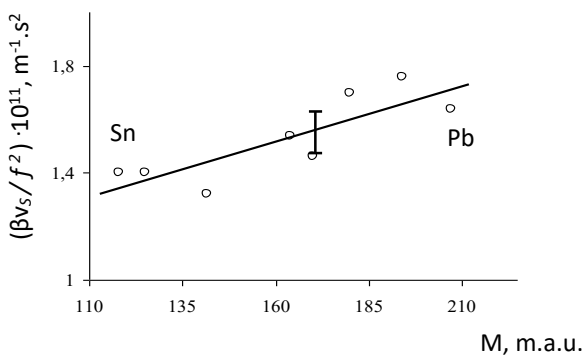$1 - \dfrac{\beta}{f^2}$, 2 - v_S

Figure 8 - Dependence for Bi-Sb system

The results in the coordinates $\dfrac{\beta v_S}{f^2} - M_A$ are shown according to Pless's data [30] for the Sn-$Pв$ system in Figure 9. Authors of this study found that the $\dfrac{\beta v_S}{f^2}$ experimental measurements are practically placed on straight lines according to Pless's experiment.

Note that the indicated results are typical only for ideal systems, that is, for melts with an atoms random distribution. We have developed an algorithm for determining the ideality or non-ideality degree of an arbitrary binary system based on monitoring the ultrasonic absorption coefficient and propagation speed experimental measurements. These are $v_S^2 - \dfrac{1}{M_A}$ and $\dfrac{\beta v_S}{f^2} - M_A$ diagrams. We study the Sn-Te system, which forms a congruently melting semiconductor chemical $SnTe$ compound. The ultrasound speed and absorption experimental measurements in the compositions $Sn_{0,30}Te_{0,70}$, $Sn_{0,5}Te_{0,5}$, $Sn_{0,70}Te_{0,30}$ are shown in Figures 10, 11, 12. The ultrasound speed and absorption for liquid tin experimental measurements are shown graphically in Figure 12.

Authors did not show a diagram for the Sn-Te system, since it was previously studied by the references [[31], [32]] in Figure 13.
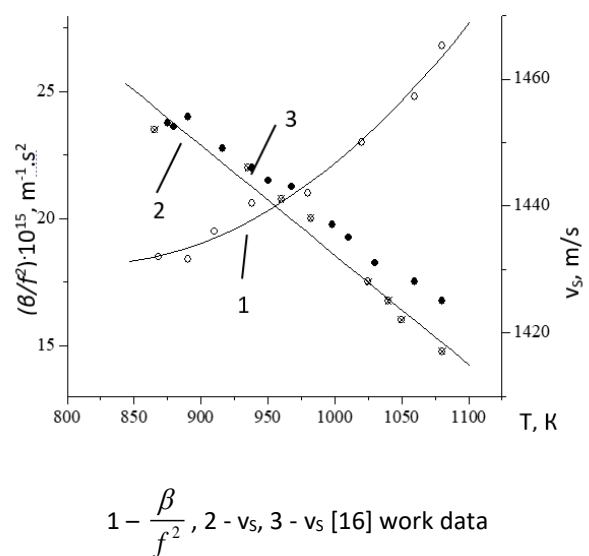
The experimental data are practically placed on straight lines in Figure 8. This confirms the closeness of the calculated indicators to the ideal ones. Indeed, the authors of the references [[28], [29]] showed that the Bi-Sb system forms a regular solutions series with atoms' random arrangement.

Figure 9 - Dependence for Sn-Pb system [17]

$1 - \dfrac{\beta}{f^2}$, 2 - v_S, 3 - v_S [16] work data

Figure 10 - Temperature dependence in $Sn_{0,30}Te_{0,70}$ melts

$$1 - \frac{\beta}{f^2}, \ 2 - v_S, \ 3 - v_S \ [16] \text{ work data}$$
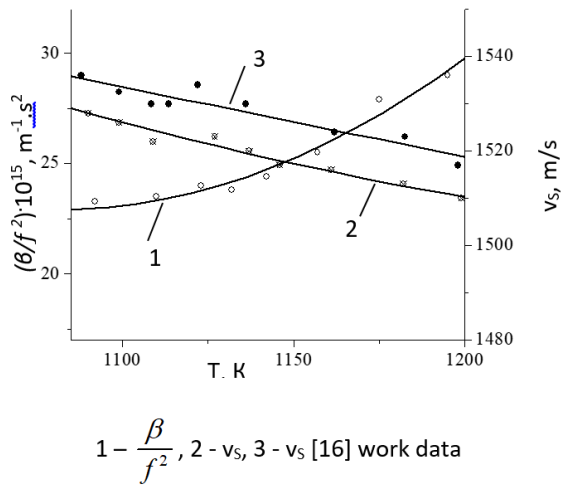
Figure 11 - Temperature dependence in $Sn_{0,5}Te_{0,5}$ melts

$$1 - \frac{\beta}{f^2}, \ 2 - v_S, \ 3 - v_S \ [16] \text{ work data}$$
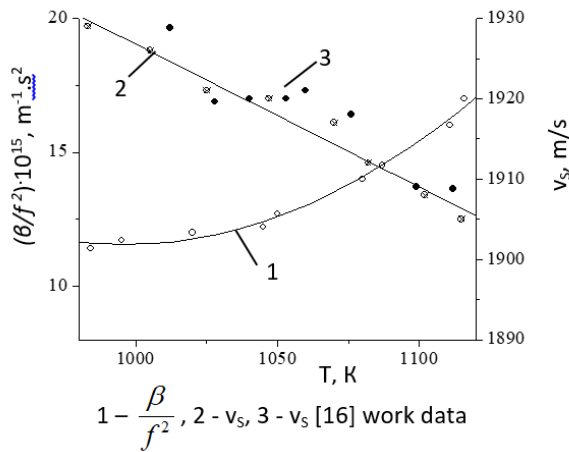
Figure 12 - Temperature dependence in $Sn_{0,70}Te_{0,30}$ melts

$$1 - \frac{\beta}{f^2}, \ 3 - v_S, \ 2 - \frac{\beta}{f^2} \ [8], \ 4 - v_S \ [16] \text{ work data}$$
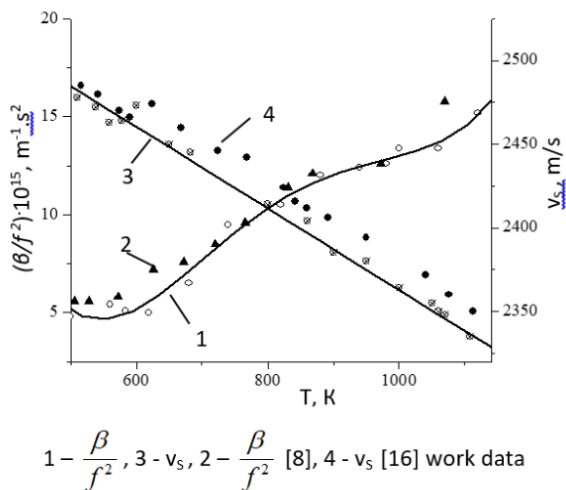
Figure 13 - Temperature dependence in liquid tin

$$1 - Sn_{0,30}Te_{0,70} \quad 2 - SnTe \quad 3 - Sn_{0,70}Te_{0,30}$$
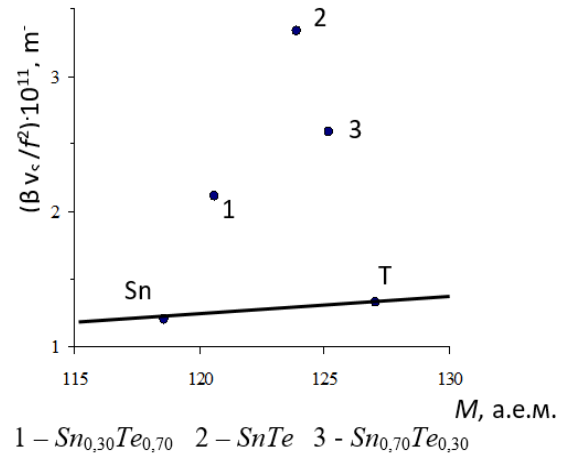
Figure 14 - Dependence for *Sn-Te* system

Calculations show that there are inconsistencies between the real isotherm and $\frac{\beta v_S}{f^2} - M_A$ linearity. Previously, for *Bi-Sb* and *Pв-Sn* systems, it was found that these deviations are associated with melt microheterogeneity of intermediate concentrations.

We have obtained a connection between the real isotherm $\frac{\beta v_S}{f^2} = f(M_A)$ and the corresponding linear diagram, which will allow us to evaluate the homogeneity or inhomogeneity of the melts and solutions.

Let us consider a melt of the *SnTe* compound stoichiometric composition. We calculate the *SnTe* experimental measurement $\frac{\beta v_S}{f^2}$ and represent it in Figure 13 with the number 2. Through this point we draw a straight line parallel to the *M* axis. Let us assume that the *SnTe* melt is atomic and calculate the average M_A atomic mass by formula (4).

An atomic *SnTe* melt corresponds to an extremely large M_A mass in an idealized system characterized by a linear dependence $\frac{\beta v_S}{f^2} - M_A$.

As a result, the atomic mass of a real melt largely exceeds the average value atomic mass of the components. This unambiguously takes place in a situation where a real *SnTe* melt consists not only atoms of tin and tellurium, but also larger particles, such as clusters or associates, whose masses exceed the component atoms masses.

System analysis based on the Periodic Law can also be applied to describe the behavior of the velocity of propagation of elastic waves in melts of simple substances. To establish such a pattern, we

analyze the Laplace equation of the following form where β_S is the adiabatic compressibility of the melt, ρ is the density.

$$v_S^2 = \frac{1}{\rho\beta_S}, \qquad (5)$$

In this case, the adiabatic compressibility of liquids from the thermodynamics point view can be represented as the reciprocal of the isothermal or adiabatic modulus of elasticity from formula where Ω is volume, P is pressure.

$$\beta_S = \frac{1}{\Omega}\frac{d\Omega}{dP}, \qquad (6)$$

Using the methods of the theory of similarity and dimension, authors of this study rewrite expression (5) in the following form:

$$\left[\frac{m^2}{s^2}\right] = \left[\frac{m^3}{kg}\right]\frac{\left[m^3\right]\cdot\left[\text{N/m}^2\right]}{\left[m^3\right]}, \qquad (7)$$

or

$$\left[\frac{m^2}{s^2}\right] = \left[\frac{m^3}{kg}\right]\frac{\left[\text{N}\cdot\text{m}^2\right]}{\left[m^3\right]}.$$

Finally

$$\left[\frac{m^2}{s^2}\right] = \frac{[J]}{[kg]}. \qquad (8)$$

From this relation, we can write the following empirical expression:

$$v_S^2 = b_1\frac{J}{M}, \qquad (9)$$

where J is the last valence electron ionization potential.

A relation like (9) makes it possible to use the ionization potentials of valence electrons to interpret the elastic properties of melts. In addition, it provides an opportunity to develop a new type diagram $v_S^2 - \frac{J}{M}$.

It should be emphasized that the use of the ionization potentials of atoms together with the Periodic Law was first applied to explain the chemical nature of substances.

In addition, the diagram $v_S^2 - \frac{J}{M}.$, supplementing the diagram $\frac{\beta v_S}{f^2} - M$, can be used to identify the number of bonds of fractal-cluster formations in melts, but this requires special consideration.

In the light of the above, authors of this study analyzed relation (9) for the experimental data on the velocity v_S^2 of ultrasonic waves in the coordinates $v_S^2 - \frac{J}{M_A}.$

When processing the experimental data by the least squares method for the series Li+, Na+, K+, Rb+, Cs+, the first ionization potential was used, and for the third group Al^{3+}, Ga^{3+}, In^{3+}, Tl^{3+}, the third ionization potential was used. In this case, the following dependence was established (Figure 15)

$$v_S^2 = 5,7\cdot10^8\left(\frac{J}{M}\right).$$

The common rectilinear arrangement for both groups is due to the fact that the outer shells of the considered ions are closed, becoming in fact isoelectronic and characteristic of hard-to-deform shells of inert gases.

The generality of the coefficient b_1 requires disclosure of the nature of its origin.

In a more general form and for further analysis of experimental data, relation (9) can be represented as

$$v_S^2 = \gamma\frac{W}{M}, \qquad (10)$$

where γ is the similarity coefficient and W is the energy of the electronic subsystem from which the ionization energy J will then be extracted.

To clarify the nature of the coefficient b_1, we represent the energy of the state of the electronic subsystem as follows:

$$|W| = Rhc\frac{z^{*2}}{n^2}, \qquad (11)$$

where z* is the effective charge of the ion, R is the Rydberg constant.

To apply Bridgman's P-theorem, we represent (11) in the following form:

$$W = \text{const} \cdot R^d \cdot h^h \cdot z^k \cdot e^l \cdot r^m \cdot c^n.$$

After finding the power coefficients, authors of this study obtain the final version of formula (11):

$$|W| = \frac{2}{2} Rhc \frac{z^2}{n^2} \cdot \frac{hc}{2\pi e^2} \cdot \frac{2\pi e^2}{hc} \cdot \frac{r}{r} \cdot \frac{2\pi e^2}{2\pi e^2},$$

and taking into account $\alpha = \dfrac{2\pi e^2}{hc}$, it can be written

$$|W| = \frac{1}{2} \cdot \frac{R\,r}{\alpha^2} \cdot F^{tr} \left[\frac{4\pi e^2}{r} \frac{z^{*2}}{n^2} \alpha \right],$$

where $F^{tr}\left[\dfrac{4\pi e^2}{r} \dfrac{z^{*2}}{n^2} \alpha \right] = J$.

The sign $F^{tr}[\quad]$ means the operator of functional transformation by the similarity method.

This expression denotes the ionization energy. Thus, the energy of the electronic subsystem $|W|$ expressed as:

$$|W| = \frac{1}{2} \cdot \frac{R\,r}{\alpha^2} J, \qquad (12)$$

taking $r \approx a_0$, and also taking into account

$$R = \frac{me^4}{4\pi\hbar^3 e}, \qquad a_0 = \frac{\hbar^2}{me^2},$$

relation (12) can be simplified to the following form

$$W = \frac{1}{8\pi\alpha} J.$$

Substituting this into (10), we obtain

$$v_s^2 = \frac{\gamma}{8\pi\alpha} \frac{J}{M}. \qquad (13)$$

Comparing this expression with (9), we find

$$b_1 = \frac{\gamma}{8\pi\alpha}.$$

Comparing this ratio with the experimental values of b_1, we can establish that $\gamma = 10+8$.

In other words, we get

$$b_1 = \frac{1}{8\pi\alpha} \cdot 10^8.$$

Table 2 and Figure 15 present the combined experimental data for the Li+ and Al³⁺ series.

As can be seen, the experimental values can be approximated by the equation of a straight line emerging from the origin,

$$v_s^2 = b_1 \left(\frac{J}{M} \right),$$

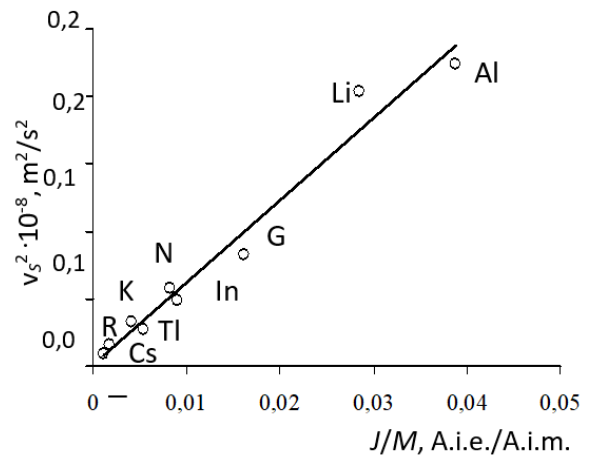where coefficient $b_1 = 5{,}7 \cdot 10^{+8}$.

Figure 15 - Experimental dependence

The reliability of the coefficient b_1 obtained from the experiment, as well as its relation to the fine structure constant, can be established by the statistical method described in [[22], [23], [24], [25], [26]].

Following the logic of these works, we write the expression for the absolute confidence interval in the following form:

$$\delta = \frac{y_{\max} - y_{\min}}{t_R},$$

where $y_{\max}$ is the maximum value of v_s^2, $y_{\min}$ is the minimum value, t_R is the significance of the correlation coefficient determined by the formula

$$t_R = \frac{R\sqrt{n-k-1}}{1-R^2},$$

where $k = 1$ is the factors number, n is the points number, R is the correlation coefficient

$$R = \sqrt{1 - \frac{(n-1)\sum(y_{\ni} - y_T)^2}{(n-k-1)\sum(y_{\ni} - y_{cp})^2}}.$$

The relative confidence interval is defined as

$$\pm \frac{\delta}{y_{midl}}, \quad \text{or} \quad \frac{\delta}{y_{midl}} b_1 - b_1 < b_1 < b_1 + \frac{\delta}{y_{midl}} b_1. \quad (14)$$

When processing the experimental data, it was found that $R = 0.97712$ at the 95% confidence level. Coefficient $t_R = 57{,}1699 \gg 2$.

Then, using the interval (14), we can write $5{,}43 \cdot 10^8 < b_1 < 5{,}97 \cdot 10^8$, whereas

$$b_T = \frac{1}{8\pi\alpha} \cdot 10^8 = 5{,}45 \cdot 10^8.$$

Table 2 - Experimental data on the series Li+ and Al³+

Ions of elements	$\dfrac{J}{M}$, $\dfrac{\text{A.i.e.}}{\text{A.i.m.}}$	v_S^2, m²/s², Experimental	v_S^2, m²/s² Theoretical
			$2.21\cdot10^7$
Al³+	0.038742994	22420000	$1.63\cdot10^7$
Li+	0.028552	20350000	$9.22\cdot10^6$
Ga³+	0.016186833	8213956	$5.11\cdot10^6$
In³+	0.008971086	4906225	$4.68\cdot10^6$
Na+	0.008213	5736025	$3.05\cdot10^6$
Tl³+	0.005358441	2608225	$2.33\cdot10^6$
K+	0.00408	3312400	$1.02\cdot10^6$
Rb+	0.001796	1587600	$6.13\cdot10^5$
Cs+	0.001076	935089	

This calculation shows that the found coefficient b_1 is within the confidence interval, which confirms the results obtained. Thus, the coefficient b_1 is also universal, as is α.

The experimental data analysis on the velocity of elastic waves based on ionization potentials and atomic mass leads to the following expression

$$v_S^2 = \gamma \frac{W}{M_A}$$

where γ = 10⁸, v_S is the ultrasonic waves speed, W is the electronic subsystem energy, equal to

$$W = \frac{1}{2} \frac{R a_0}{\alpha^2} F^{tr} \left[\frac{\alpha}{n^2} \frac{4\pi}{r} z^{*2} e^2 \right].$$

Here α is the fine structure constant, e is the charge, r is the interion distance, n is the effective quantum number, a_0 is the radius, z^* is the free electrons number per atom.

As noted earlier, sign $F^{tr}[\;\;]$ means a functional transformation operator.

v_S^2 is represented in the form, according to the Laplace formula,

$$v_S^2 = \frac{1}{\beta_S \rho},$$

Or with $\rho = \dfrac{m}{V} = \dfrac{N_A M_A}{N_A V_A}$, $v_S^2 = \dfrac{V_A}{\beta_S} \dfrac{1}{M_A}$.

Let us designate as the connection factor

$$\frac{1}{b_S} = \frac{V_A}{\beta_S}.$$

On the other hand, heating leads to an increase in the number of free electrons, so to a change in the short-range order in the structure of the melt.

In other words, the elements of anisotropy in the short-range order are destroyed in the molten state, thereby an electronic and ionic subsystem rises. An increase in the number of free electrons, metallizing bonds, leads to a decrease in compressibility. Therefore, for the metals' compressibility, one can give the Ya.I. Frenkel formula:

$$\beta_S = \frac{18r^4}{A\,z^{*2}e^2}, \qquad (15)$$

where r is the interion distance, A is the Madelung constant, z^* is the free electrons number per atom, and e is the electron charge.

The formula (15) taking into account the ionic volume can be represented as follows for the further analysis convenience

$$\beta_S = \frac{432V'r}{4\pi\,Az^{*2}e^2}.$$

We can write passing from $β_S$ to $\dfrac{1}{b_S}$

$$\frac{1}{b_S} = \frac{4\pi\,Az^{*2}e^2}{432V'r}.$$

Because

$$\frac{1}{b_S} = \gamma\,W = \frac{1}{2} \frac{R a_0}{\alpha^2} F^{tr} \left[\frac{4\pi\,z^{*2}e^2}{r} \alpha \frac{1}{n^2} \right]$$

assuming the multiplicity of factors $F^{tr}[\;\;]$ and equating

$$\frac{1}{b_S} = \frac{V_A}{V'} \frac{A}{432} \frac{4\pi}{r} z^{*2}e^2$$

and

$$\frac{1}{b_S} = \frac{1}{2} \frac{R a_0}{\alpha} \frac{4\pi}{r} z^{*2}e^2 F^{tr}\left[\frac{1}{n^2}\right],$$

can be installed

$$\frac{R a_0}{\alpha} F^{tr}\left[\frac{1}{n^2}\right] = \frac{A}{216} \frac{V_A}{V'}.$$

Thus, we can consider the connection between α and the Madelung constant to be established. This suggests that, at high densities of matter, elastic waves exhibit quantum properties, not to mention phonon-phonon interactions.

Conclusions

The practical value of direct acoustic measurements and feasibility in liquid metals in this work is demonstrated. These investigations can be used for ultrasonic melt processing optimization. The physical and chemical ultrasound effects on liquid melts structure were investigated. We determined that the chemical effect is an irreversible and permanent change in atom weight and the atom-weight distribution due to ultrasound in our study with specific components and ultrasound system. As the ultrasound intensity increases, the atom weight of liquid metals reduces and its atom-weight distribution becomes narrower; the liquid metals atom orientation along the flow direction reduces (in melt state). Ultrasound vibration increases the atom chains motion and makes them more disorder; it also affects the liquid metals relaxation process, leading to weakening the elastic effect.

The absorption, propagation speed temperature dependences, and compressibility of simple semimetals, semiconductors, and semiconductor compounds have been theoretically studied.

Experimental and theoretical results testify to the microheterogeneity of semimetals and semiconductors melts.

Generalization and analysis of experimental data on absorption and propagation speed on the Laplace equation basis and the D.I. Mendeleev periodic law unambiguously indicate the presence of microgroups of atoms (clusters) microheterogenizing semimetals and semiconductors melts.

The nature analysis of the v_s and α polytherms can be concluded from the literature data that a wide temperature range for the manifestation of anomalies in these properties is associated with the coexistence of metallic and interatomic bonds covalent types in the considered melts, which is inherent in clusters.

Semiconductor melts are separated into a separate class of electronic melts. The whole set of experimental data on viscosity, density, and electrical properties, as well as the results of structural studies show that this electron melts class exhibits changes in the short-range order structure upon heating. Therefore, anomalies and features of the melts of semimetals and semiconductors' acoustic properties should be considered manifestations of structural changes.

It is known that the fine structure constant α determines the relationship between electromagnetic and weak interactions, combining them into one theory. The results obtained above emphasize its connection with the elastic wave characteristics since the elastic properties of matter also have a wave nature, as well as electroweak interactions.

Сұйық металдардағы акустикалық өлшемдердің техникалық және практикалық мәнін көрсету

¹Қажыкенова С.Ш. , ¹Шайхова Г.С. , ¹Шалтақов С.Н. , ²Беломестный Д.

¹Абылқас Сағынов Қарағанды техникалық университеті, Қарағанды, Қазақстан
² Дуйсбург – Эссен университеті, Дуйсбург, Германия

ТҮЙІНДЕМЕ

Бұл жұмыста қарапайым жартылай металдардағы, жартылай өткізгіштердегі және жартылай өткізгіш қосылыстардағы ультрадыбыстың жұтылу және таралу жылдамдығының температураға тәуелділіктері зерттелген. Тәжірибелік және теориялық нәтижелер жартылай металдар мен жартылай өткізгіш балқымалардың микрогетерогенділігін дәлелдейді. Балқымалардағы ультрадыбыстың жұтылу және таралу жылдамдығы бойынша тәжірибелік деректерді Д.И. Менделеевтің периодтық заңы негізінде қорыту және талдау оларда жартылай металдар мен жартылай өткізгіштердің балқымаларын микрогетерогендейтін атомдар (кластерлер) микротоптарының болатындығын анық көрсетеді. Бұл мәселенің өзектілігі заттың сұйық күйі мәселесімен анықталады. Ультрадыбыстың сіңіру және таралу жылдамдығының температураға тәуелділігі осы жұмыстағы үлгілердің бірнеше тобын пайдаланып өлшенеді, әр топ әртүрлі температураға дейін қызады. Жартылай өткізгіштік қасиеті бар балқымалардың, олардың атомдық матрицасында шоғырлардың болуына байланысты, микробіртекті емес екендігі дәлелденді. Бұл нәтижелер жаңа құнды идеяларды, соның ішінде балқытуды ультрадыбыспен өнеркәсіптік масштабқа дейін масштабтау үшін қажет идеяларды тудырып отыр.

Түйінді сөздер: балқымалар, атомдық масса, ультрадыбыстық балқыма, ультрадыбысты сіңіру, температураға тәуелділік, ультрадыбыстың таралу жылдамдығы.

Авторлар туралы ақпарат:

Кажикенова Сауле Шарапатқызы
Техника ғылымдарының докторы, профессор, Абылқас Сағынов Қарағанды техникалық университетінің «Жоғары математика» кафедрасының меңгерушісі, Қарағанды, Қазақстан. Email: sauleshka555@mail.ru

Шаихова Гүлназира Серікқызы
Техника ғылымдарының кандидаты, Абылқас Сағынов Қарағанды техникалық университетінің «Жоғары математика» кафедрасының доцентінің м.а., Қарағанды, Қазақстан. Email: shaikxova_2011@mail.ru

Шалтаков Сағындык Нағашибайұлы
PhD, Абылқас Сағынов Қарағанды техникалық университетінің «Физика» кафедрасының аға оқытушысы, Қарағанды, Қазақстан. Email: sagyndyk613@mail.ru

Беломестный Денис
PhD, Дуйсбург-Эссен университетінің профессоры. Email: denis.belomestny@uni-due.de

Демонстрация возможности и практической ценности прямых акустических измерений в жидких металлах

[1]Кажикенова С.Ш. , [1]Шаихова Г.С. , [1]Шалтаков С.Н. , [2]Беломестный Д.

[1] Карагандинский технический университет имени Абылкаса Сагинова, Караганда, Казахстан
[2]Университет Дуйсбург – Эссена, Дуйсбург, Германия

АННОТАЦИЯ

В работе исследованы температурные зависимости поглощения и скорости распространения ультразвука в простых полуметаллах, полупроводниках и полупроводниковых соединениях. Экспериментальные и теоретические результаты свидетельствуют о микрогетерогенности расплавов полуметаллов и полупроводников. Обобщение и анализ экспериментальных данных по поглощению и скорости распространения ультразвука в расплавах на основе Периодического закона Д.И. Менделеева четко указывают на наличие в них микрогрупп атомов (кластеров), микрогетерогенизирующих расплавы полуметаллов и полупроводников. Актуальность этой проблемы предопределена проблемой жидкого состояния вещества. Зависимость поглощения и скорости распространения ультразвука от температуры измеряется с использованием нескольких групп образцов в настоящей работе, каждая группа нагревается до разной температуры. Доказано, что расплавы с полупроводниковыми свойствами являются микронеоднородными из-за наличия в их атомной матрице кластеров. Эти результаты дают ценные новые идеи и идеи, необходимые для масштабирования обработки расплава ультразвуком в промышленных масштабах.

Ключевые слова: расплавы, атомная масса, ультразвуковой расплав, поглощение ультразвука, температурные зависимости, скорость распространения ультразвука.

Информация об авторах:

Кажикенова Сауле Шарапатовна
Доктор технических наук, профессор, заведующая кафедрой «Высшая математика», Карагандинский технический университет имени Абылкаса Сагинова, Карганда, Казахстан. E-mail: sauleshka555@mail.ru

Шаихова Гульназира Сериковна
Кандидат технических наук, и.о.доцента кафедры «Высшая математика», Карагандинский технический университет имени Абылкаса Сагинова, Караганда, Казахстан. E-mail: shaikxova_2011@mail.ru

| Шалтаков Сагындык Нагашибаевич | *PhD, старший преподаватель кафедры «Физика», Карагандинский технический университет имени Абылкаса Сагинова, Караганда, Казахстан. E-mail: sagyndyk613@mail.ru* |
| Беломестный Денис | *PhD, Профессор Университета Дуйсбург-Эссен, Дуйсбург, Германия. E-mail: denis.belomestny@uni-due.de* |

Reference

[1] YAO T, KONDIC V. Viscosity of Metallic Liquids. Nature. 1950; 166:483. https://doi.org/10.1038/166483a0

[2] Brenman M, Nuthinson P, Sandster ML, Schosieid P. Calculation of an effective pair interaction potential for Liquid neon from structure factor measuvements. J. Phys. C. Solid State Phys. 1974; 7(23):411-414.

[3] Havel J, Meloun M. Multiparametric curve fitting. Part. 9, Simultaneous regression estimation of stechiometry and stability constants of complexes. Talanta. 1986; 33(5):435-441. https://doi.org/10.1016/0039-9140(86)80111-4

[4] Mitra SK, Nuthinson P, Sandster ML, Schosieid PA. Pair interaction potential for rubidium calculated from thermodynamic and neutron diffraction data. Philos. 1976; 34(6):1087-1100.

[5] Bloek R, Sush IB, Blaser W, et. al. Measurement of the structure faeton of Liquid rubidium by neutron diffraction up to 1400 K and 200 bar. Ber. Bunsenges. Phys. Chem. 1976; 80(8):718-774.

[6] Regel AR, Glazov VM. Periodic law and physical properties of electronic melts. M.: Nauka. 1982, 296.

[7] Poltavtsev YuG. Struktura poluprovodnikovykh rasplavov [Structure of semiconductor melts]. Moscow: Metallurgy. 1984, 176. (in Russ.).

[8] Chinnam RK, Fauteux C, Neuenschwander J, Janczak-Rusch J. Evolution of the microstructure of Sn–Ag–Cu solder joints exposed to ultrasonic waves during solidification. Acta Materialia. 2011; 59(4):1474-1481. https://doi.org/10.1016/j.actamat.2010.11.011

[9] Kazhikenova SSh, Shaltakov SN, Nussupbekov B. Difference melt model. Archives of Control Sciences. 2021; 31(LXVII):607-627. https://doi.org/10.24425/acs.2021.138694

[10] Mesaros M, Martínez OE, Bilmes GM, Tocho JO. Acoustic detection of laser induced melting of metals. J. Appl. Phys. !997; 81(2):1014-1016. https://doi.org/10.1063/1.364196

[11] Hackett L, Miller M, Weatherred S. Non-reciprocal acoustoelectric microwave amplifiers with net gain and low noise in continuous operation. Nat Electron. 2023; 6:76-85. https://doi.org/10.1038/s41928-022-00908-6

[12] White DL. Amplification of ultrasonic waves in piezoelectric semiconductors. J. Appl. Phys. 1962; 33:2547-2554.

[13] Eskin DG, Tzanakis I, Wang F, Lebon GSB, Subroto T, Pericleous K, Mi J. Fundamental studies of ultrasonic melt processing. Ultrasonics Sonochemistry. 2019; 52:455-467. https://doi.org/10.1016/j.ultsonch.2018.12.028

[14] Kamioka H. Behavior of Tin-Bismuth alloys near melting point found by measurement of sound velocity. J. Phys. Soc. Jap. 1984; 53(4):1349-1355.

[15] Gitis MB, Mikhailov IG, Niyazov S. Sound absorption in liquid sulfur. Acoust. Journal. 1970; 16(3):472-473.

[16] Gallego LJ, Rey C, Crimson MJ. A Monte Carlo simulation study of the disjoining pressure in thin fluid films stercally stabilized by terminally attached chains. Mol. Phys. 1991; 74(2):383-395.

[17] Abowitz G, Gordon RB. Internal friction in metals: mercury and mercury-thallium Alloys. Acta metal. 1962; 10(7):671-679.

[18] Jarzynski L, Litovitz TA. Ultrasonic absorption in Liquid Sodium-Potassium alloys. J. Chem. Phys. 1964; 41(5):1290-1296.

[19] Reing EN, Beyer RT. Ultrasonic absorption in liquid selenium. J. Acoust. Soc. Amer. 1977; 62(3):582-588.

[20] Aider JL, Wesfreid JE. Characterisation of Longitudinal Görtler Vortices in a Curved Channel Using Ultrasonic Doppler Velocimetry and Visualizations. J. Phys. 1996; 6(7)893-906. https://doi.org/10.1051/jp3:1996162

[21] García-Colín LS, De La Selva SMT. The Stokes-Kirchhoff relation in chemically reacting fluids. Chemical Physics Letters. 1973; 23(4):611-613. https://doi.org/10.1016/0009-2614(73)89041-4

[22] Shekaari H, Golmohammadi B. Ultrasound-assisted of alkali chloride separation using bulk ionic liquid membrane. Ultrasonics Sonochemistry. 2021; 74:105549. https://doi.org/10.1016/j.ultsonch.2021.105549

[23] Liu Y, Yu W, Liu Y. Effect of ultrasound on dissolution of *Al* in *Sn*. Ultrasonics Sonochemistry. 2019; 50:67-73. https://doi.org/10.1016/j.ultsonch.2018.08.029

[24] Zheng Y, Yi Tan X, Xiaojuan Wan, Cheng X, Liu Zh, Yan Q. Thermal stability and mechanical response of Bi_2Te_3 - based materials for thermoelectric applications. ACS Applied energy materials. 2020; 3(3):2078-2089. https://doi.org/10.1021/acsaem.9b02093

[25] Chiba A, Ohmasa Y, Yao M. Vibrational, single-particle-like, and diffusive dynamics in liquid *Se, Te*, and $Te_{50}Se_{50}$. J. Chem. Phys. 2003; 119(17):9047-9062. https://doi.org/10.1063/1.1615234

[26] Inui M, Kajihara Y, Tsuchiya Y. Peculiar temperature dependence of dynamical sound speed in liquid $Se_{50}Te_{50}$ by inelastic x-ray scattering. Journal of Physics Condensed Matter. 2020; 32(21):214003. https://doi.org/10.1088/1361-648X/ab6d8e

[27]   Shleifer F, Wilson JD, Loring R. Self-consistent theory of polymer dynamic in melts. J. Chem. Phys. 1991; 95:8474-8485. https://doi.org/10.1063/1.461277

[28]   Liu JM, Wu WH, Zhai W, Wei B. Ultrasonic modulation of phase separation and corrosion resistance for ternary *Cu-Sn-Bi* immiscible alloy. Ultrasonics Sonochemistry. 2019; 54:281-289. https://doi.org/10.1016/j.ultsonch.2019.01.029

[29]   Kuliev BB, Rustamov PG, Aliyanov MA, Kuliev EM. Ultrasonic studies on the interaction of SnTe-InTe systems. Physica Status Solidi (a). 1971; 4(2):127-130. https://doi.org/10.1002/pssa.2210040241

[30]   Pless KG. Ultrasonic measurements in metals in the molten state and upon unsolidification [Ultraschallmessungen in metallen im Geschmolzenen zustand und Beim Enstarren]. Acustica. 1963; 3:240-244. (in Ger.).

[31]   Inui M, Kajihara Y, Hosokawa Sh, Matsuda K, Tsuchiya Y. Dynamical sound speed and structural inhomogeneity in liquid *Te* studied by inelastic x-ray scattering. Journal of Non-Crystalline Solids. 2019; 1: 100006. https://doi.org/10.1016/j.nocx.2018.100006

[32]   Yu W, Liu Y, Liu Y, Formation and Evolution of Cu-Sn Intermetallic Compounds in Ultrasonic-Assisted Soldering. J. Electron. Mater. 2019; 48:5595-5602. https://doi.org/10.1007/s11664-019-07405-1